Significance of Binding to Na,K-ATPase in the Tissue Distribution of Ouabain in Guinea Pigs

Hideyoshi Harashima,[1,2] Michio Mamiya,[1,3] Masayo Yamazaki,[1] Yuichi Sugiyama,[1,6] Yasufumi Sawada,[1,4] Tatsuji Iga,[1,4] and Manabu Hanano[1,5]

Received June 28, 1991; accepted October 30, 1991

Ouabain binds specifically to Na,K-ATPase on the plasma membrane and therefore serves to measure the tissue concentration of Na,K-ATPase. We examined the role of ouabain binding to Na,K-ATPase in its overall tissue distribution. The tissue-to-plasma concentration ratio ($K_{p,vivo}$) was defined in each tissue after intravenous administration of ^{3}H-ouabain in guinea pigs, and specific binding of ouabain to Na,K-ATPase was measured in tissue homogenate to obtain the dissociation constant and binding capacity in each tissue. A predicted tissue-to-plasma concentration ratio ($K_{p,vitro}$) was calculated using the obtained binding parameters and the volume of extracellular space in each tissue. The absolute values of $K_{p,vitro}$ were comparable to those of $K_{p,vivo}$, except in brain. Regression analysis showed that the specific binding capacity of Na,K-ATPase in each tissue is the main factor in the tissue variation of $K_{p,vivo}$. Therefore, the binding of ouabain to Na,K-ATPase plays a significant role in the tissue distribution of ouabain.

KEY WORDS: cardiac glycosides; ouabain; Na,K-ATPase; guinea pig; tissue distribution; tissue-to-plasma concentration ratio.

INTRODUCTION

Since the introduction of physiological pharmacokinetic model by Bishoff and Dedrick (1,2), the validity of this concept has been examined and applied to many drugs (3,4). Animal scale-up is one of the important applications of this concept (5). When we evaluate drug effect and toxicity, drug concentration in tissue is important; however, it is usually difficult to measure tissue concentrations in human. The physiological model can predict the time courses of tissue concentrations provided that the tissue-to-plasma partition coefficients (K_p value) in humans are given. Therefore, it is important to develop a method to predict K_p values in human based on animal experiments.

Sawada *et al.* revealed that the determinant factor of species differences in the distribution volume of basic drugs is the plasma unbound fraction (f_p), and there is no interspecies variation in the distribution volume of unbound drugs (6). For doxorubicin, the tissue concentration of DNA was shown to determine the tissue distribution (7). In such cases, the prediction of tissue distribution based on the physiological model should be improved.

In the case of cardiac glycosides, there is a large species variation in tissue distribution. The volume of distribution for digoxin is 3.7 (L/kg) in rats (8), 5.3 (L/kg) in guinea pigs (9), 9.1 (L/kg) in dogs (10), 9.7 (L/kg) in human (10), and 20.4 (L/kg) in cats (10). Variation in the unbound fraction of digoxin cannot account for this variation in the volume of distribution. Harrison and Gibaldi made a physiological model of digoxin distribution in the rat (11), however, the K_p values in rats were too small to extrapolate to the human. Therefore, they constructed a physiological model in dogs, which have a similar volume of distribution, and predicted the tissue concentration in humans based on the K_p values of dogs (12). If one had known the variation factor(s) in the tissue distribution of cardiac glycosides quantitatively, the prediction could be made in a more rational manner.

Cardiac glycosides bind specifically to Na,K-ATPase, which is considered to be its pharmacological receptor (13). There are many studies on the species differences in the specific binding of ouabain to isolated Na,K-ATPase, and this variation correlates well with the species difference in cardiac glycosides sensitivity (14–16); however, little is known about the role of binding to Na,K-ATPase in the tissue distribution of cardiac glycosides. In this study, we selected ouabain as a model cardiac glycoside to examine the significance of the binding to Na,K-ATPase in the tissue distribution, because ouabain is not metabolized and does not bind to plasma proteins.

METHODS

Materials. Ouabain was purchased from Sigma Chemical Co. (St. Louis, MO). ^{3}H-Ouabain (20 Ci/mmol) was obtained from New England Nuclear (Boston, MA). The radioactive compound was confirmed to be at least 98% pure by thin-layer chromatography (TLC) with chloroform/methanol/water (65:30:5). All other chemicals were of analytical grade.

In Vivo *Distribution Study.* All experiments were performed using male Hartley guinea pigs weighing 250–400 g from Nihon Igaku Doubutsu (Tokyo). Each animal was anesthetized with ethyl carbamate (urethane; 600 mg/kg) and α-chloralose (60 mg/kg) ip. Body temperature was kept at 37°C using a heat lamp during study. The jugular vein and carotid artery were cannulated with polyethylene tubing (PE-50) for drug infusion and blood sampling, respectively. Ouabain was infused at the rate of 10 nmol/min/kg body weight, using an infusion pump (Model 975E, Harvard Ap-

[1] Faculty of Pharmaceutical Sciences, University of Tokyo, Hongo, Bunkyo-ku, Tokyo 113, Japan.
[2] Present address: Faculty of Pharmaceutical Sciences, University of Tokushima, 1-78-1, Shomachi, Tokushima, 770, Japan.
[3] Present address: Shionogi and Co., Ltd., Shionogi Research Laboratories, 2-1-3, Kuise-Terashima, Amagasaki City, Hyogo 660, Japan.
[4] Present address: Department of Pharmacy, University of Tokyo Hospital, Faculty of Medicine, University of Tokyo, Hongo, Bunkyo-ku, Tokyo 113, Japan.
[5] Present address: College of Pharmacy, Nihon University, 7-7-1, Narawashinodai, Funabashi City, 274, Japan.
[6] To whom correspondence should be addressed.

0724-8741/92/0400-0474$06.50/0

paratus, South Natick, MA). ^{3}H-Ouabain was infused at a rate of 3–8 μCi/min depending on the body weight. The flow rate of the solution ranged from 50 to 150 μl/min. Approximately 150 μl of blood sample was obtained at 2, 5, 10, 20, 65, 245, and 725 min after the initiation of infusion and plasma was separated by centrifugation (Beckman Instruments, Fullerton, CA). Animals were sacrificed by an injection of air through arterial cannula, and the following tissues were sampled, excised, blotted, and stored at −20°C for assay: small intestine, kidney, liver, heart, muscle (femoral), lung, and brain.

Assay. Fifty microliters of plasma was mixed with 10 ml of Biofluor, a high-efficiency emulsifier cocktail (New England Nuclear), and the radioactivity was determined in a liquid scintillation counter (Model 3255, Packard Instruments Corp., Downers Grove, IL). Quenching was determined using automatic external standardization.

A 100-mg aliquot of each tissue was sampled and 1 ml of Protosol, a tissue solubilizer (New England Nuclear), was added. The samples were heated for 6 hr at 55°C. Then 200 μl of 30% hydrogen peroxide was added to decolorize the samples. The radioactivity was determined after the chemiluminescence of control samples was less than 60 cpm. The counting efficiency was determined by the external standard method. The apparent tissue-to-plasma concentration ratio *in vivo* ($K_{p,vivo}$) was obtained by averaging K_p from 65 to 720 min.

Ouabain Binding to Na,K-ATPase in Each Tissue Homogenate. Specific binding of ouabain was measured by the rapid filtration technique basically reported by us previously (17). Ten percent of each tissue homogenate was prepared with a Teflon homogenizer with a ninefold volume of buffer containing 50 m*M* Tris–HCl, 100 m*M* NaCl, and 2.5 m*M* $MgCl_2$. The binding reaction was initiated by the addition of 50-μl aliquots of 10% homogenate to 950 μl of the incubation mixture containing 50 m*M* Tris–HCl (pH 7.4), 100 m*M* NaCl, 2.5 m*M* Na_2ATP, 2.5 m*M* $MgCl_2$, and 10 n*M* ^{3}H-ouabain (final homogenate concentration, 0.5%). To measure the concentration dependency of ouabain-specific binding, unlabeled ouabain was added to the incubation mixture up to 3000 n*M* (final concentration), which had been preincubated for 10 min at 37°C. After 30 min of incubation, aliquots (400 μl) were removed and filtered through a 0.45-μm Millipore filter (Millipore Corp., Bedford, MA) and rinsed twice with 4 ml of ice-cold (4°C) saline. The filters were dissolved in 10 ml of scintillation fluid [toluene (1 liter), Triton X-100 (0.5 liter), 1,4-bis-2-(5-phenyloxazol) benzen (0.1 g), and diphenyloxazole (4 g)] and the radioactivity was measured in a liquid scintillation counter. Specific binding was expressed by subtraction of the nonspecific binding activity in the presence of 500 μ*M* unlabeled ouabain from the total binding activity. In this experimental condition, the unbound concentration remained unaffected by its reaction with the receptor, because the bound concentration of ^{3}H-ouabain was less than 1% of the total concentration.

Pharmacokinetic Analysis of Plasma Concentration of Ouabain. The time course of ouabain concentration in plasma was fitted by the following equation using the nonlinear least-squares method (18), using the Damping Gauss Newton method with the weight of (plasma concentration)$^{-2}$.

$$0 < t < 5: \quad C_p = \sum_i^3 A_i\{1 - \exp(-a_i * t)\} \tag{1a}$$

$$5 \leqq t: \quad C_p = \sum_i^3 A_i\{1 - \exp(-a_i * 5)\} \exp\{-a_i(t - 5)\} \tag{1b}$$

where A_i and a_i are the hybrid pharmacokinetic constants. Pharmacokinetic parameters were calculated according to the following equations (19).

$$\text{AUC} = \int_0^\infty C_p dt = 5 * \sum_i^3 A_i \tag{2}$$

$$\text{AUMC} = \int_0^\infty t \cdot C_p dt = 5 * \sum_i^3 A_i(5/2 + 1/a_i) \tag{3}$$

$$\text{CL}_{tot} = \text{dose/AUC} \tag{4}$$

$$\text{MRT} = \text{AUMC/AUC} \tag{5}$$

$$V_{d\,ss} = \text{CL}_{tot} * \text{MRT} \tag{6}$$

In Vitro *Binding Parameters of Ouabain to Na,K-ATPase.* The dissociation constant (K_d; n*M*) and binding capacity (B_{max}; nmol/L of 0.5% homogenate) of ouabain in 0.5% each tissue homogenate was obtained by the nonlinear least-squares method (18) based on the following equation:

$$C_b = B_{max} \cdot C_f/(K_d + C_f) \tag{7}$$

where C_f is the free or unbound concentration.

Construction of $K_{p,vitro}$. $K_{p,vitro}$ was constructed based on the following equation, using *in vitro* binding parameters and extracellular space as described previously (17).

$$K_{p,vitro} = V_e/V_t + d \cdot B_{max}/(K_d + C_p) \tag{8}$$

where V_e, V_t, and d represent the volume of extracellular space, whole tissue volume, and dilution factor, respectively. If $K_d \gg C_p$, then $K_{p,vitro}$ can be described as follows:

$$K_{p,vitro} = V_e/V_t + d \cdot B_{max}/K_d \tag{9}$$

The ratio of extracellular space to the whole tissue volume was obtained from the literature (20), assuming that guinea pigs have the same V_e/V_t values as those of rats. The dilution factor d was 200 in this study.

Regression Analysis of $K_{p,vivo}$ *by* V_e/V_t, K_d, B_{max}, *and* $K_{p,vitro}$. Linear regression analysis was performed on V_e/V_t, $K_{p,vivo}$ by K_d, B_{max}, and $K_{p,vitro}$ based on the following equation to examine the determinant factor of $K_{p,vivo}$:

$$K_{p,vivo} = a + b \cdot P \tag{10}$$

where a and b are regression coefficients and P is an independent variable such as K_d, B_{max}, and $K_{p,vitro}$.

RESULTS

In Vivo *Tissue Distribution Study*. The time course of the plasma concentration of ouabain is shown in Fig. 1. The concentrations increased for the first 5 min, then rapidly decreased up to 65 min, then decreased slowly. The time profile of the averaged plasma concentration was fitted to Eqs. (1a) and (1b). The pharmacokinetic parameters were calculated according to Eqs. (2)–(6) and are summarized in Table I. Total body clearance was 7.06 (ml/min/kg), which was explained mainly by the glomerular filtration rate (7.81 ml/min/kg) (21). The urinary recovery of ouabain in this study was at least 80%. The volume of distribution at steady state was 2780 (ml/kg), which was much larger than the volume of extracellular space. The time courses of ouabain concentration and K_p values in several tissues are shown in Fig. 2. Lung had a peak concentration at 5 min (end of infusion), while other tissues such as muscle (20 min), kidney (20 min), liver (20 min), GI (20 min), heart (10 min), and brain (10 min) had peak concentrations at a later time. The order of tissue concentration of ouabain is as follows: kidney > heart > GI > liver > lung > muscle > brain. Kidney had the highest $K_{p,vivo}$; on the other hand, brain had the lowest (Table I). In most of the tissue, the $K_{p,vivo}$ values increase up to 65 min and stay relatively constant after that.

Ouabain Binding to Na,K-ATPase in Each Tissue Homogenate. In each tissue, the specific binding of ouabain showed saturation with the increase in ouabain concentration and this binding was described by the single-binding site model [Eq. (7)] below 1000 n*M*. Above this concentration, the binding to a secondary site has to be taken into consideration in some tissues. The contribution of this low-affinity site (secondary site) may be negligible in this study, considering that the plasma concentration ranged from 2 to 200 n*M* (Fig. 1). We considered that this binding to the high-affinity site is specific to Na,K-ATPase, based on the following experimental evidence, which is commonly used as criteria for the binding specificity (13): (i) ^{3}H-ouabain binding in each homogenate is displaced by the cold ouabain in a concentration-dependent manner; (ii) nonspecific binding, which is not displaced by the excess cold ouabain is between 1 and 10% of the total bound radioactivities depending on the tissue; and (iii) this ^{3}H-ouabain binding is dependent on ATP and inhibited by potassium. The binding parameters are summarized in Table II. The binding experiment could not be performed for GI, because the Millipore filter could not be rinsed within 10 sec due to the high viscosity of the incubation mixture with homogenate. The dissociation constant for each tissue ranged between 130 and 630 n*M;* on the other hand, the binding capacity exhibited greater intertissue differences and ranged from 1.3 to 22 nmol/L of 0.5% homogenates.

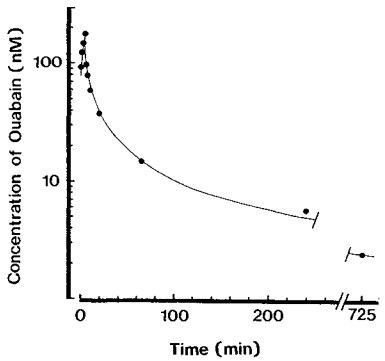

Fig. 1. Time course of plasma concentration of ouabain in guinea pigs. ^{3}H-Ouabain was infused for 5 min at a rate of 10 nmol/min/kg. Standard error is included in the symbol. Solid line represents the fitting curve based on the three-compartment model. (See Method.)

Table I. Pharmacokinetic Parameters of Ouabain in Guinea Pigs

(A) Plasma disappearance curve of ouabain[a]

A_1 (n*M*)	114	± 8
A_2 (n*M*)	345	± 28
A_3 (n*M*)	956	± 31
a_1 (min^{-1})	1.06	± 0.1
a_2 (min^{-1})	0.0350	± 0.0035
a_3 (min^{-1})	0.00176	± 0.00021
AUC (n*M* min)	7080	
AUMC (μ*M* min)	2790	
CL_{tot} (ml/min/kg)	7.06	
MRT (min)	393	
V_{dss} (ml/kg)	2780	

(B) Tissue distribution of ouabain

Tissue	$K_{p,vivo}$[b]	V_t (ml/kg)[c]	$K_{p,vivo} \cdot V_t$ (ml/kg)
Kidney	12.00 ± 0.66	8.0	96.0
Heart	4.24 ± 1.11	4.0	17.0
Muscle	4.01 ± 2.09	500.0	2005.0
G.I.	3.63 ± 0.46	44.4	161.0
Liver	2.14 ± 1.02	44.0	94.2
Lung	0.88 ± 0.28	4.8	4.2
Brain	0.18 ± 0.14	4.8	4.8
Total			2378.2

[a] Time course of plasma concentration was fitted to Eqs. (1a) and (1b), and each hybrid parameter was obtained by the nonlinear least-squares method (18) with the standard deviation. Pharmacokinetic parameters were calculated according to Eqs. (2)–(6).
[b] The $K_{p,vivo}$ values were obtained by averaging those from 65 to 720 min and are shown with standard error.
[c] Each tissue volume referred to the literature (24,25).

Regression Analysis of $K_{p,vivo}$ *by* V_e/V_t, K_d, B_{max}, *and* $K_{p,vitro}$. The results are summarized in Table III. R^2 represents the coefficient of determination, which measures the fraction of the variability of $K_{p,vivo}$ accounted for by its least-squares linear regression on P. Both the volume of extracellular space and the dissociation constant explained only 30% of the variation and the regression was not significant. On the other hand, B_{max} explained 90.9% of the variation and the regression was significant ($P < 0.025$). This result indicates that the tissue variation of $K_{p,vivo}$ comes from the diversity of the tissue concentration of Na,K-ATPase. In addition, we attempted the construction of $K_{p,vitro}$ in each tissue based on the binding parameters and the volume of extracellular space [Eqs. (8) and (9)]. The $K_{p,vitro}$ values thus constructed were compared with the $K_{p,vivo}$ values (Table IV). There is a fairly good correspondence between $K_{p,vivo}$ and $K_{p,vitro}$ except in brain. The

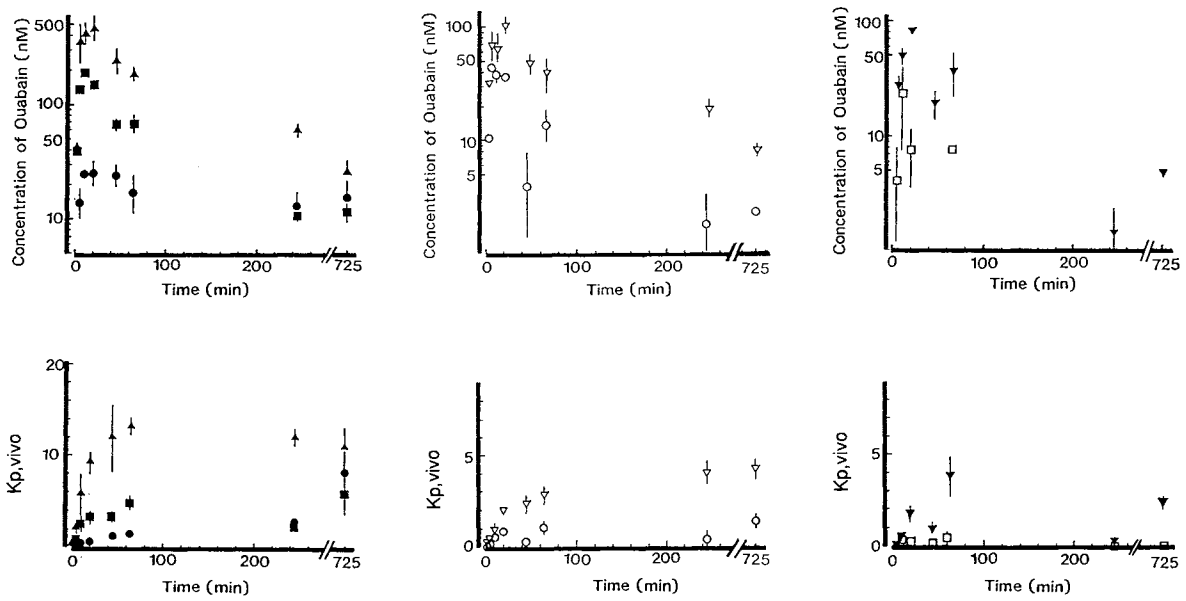

Fig. 2. Time courses of tissue concentration (top) and $K_{p,vivo}$ (bottom) of ouabain. Each tissue concentration was measured after the constant infusion of ^{3}H-ouabain at a rate of 10 nmol/min/kg for 5 min. Vertical bar represents standard error (n = 3). (●) Muscle; (■) heart; (▲) kidney; (○) lung; (▽) GI; (□) brain; (▼) liver.

$K_{p,vitro}$ had the highest coefficient of determination (R^2) and the regression was significant ($P < 0.01$).

DISCUSSION

The pharmacokinetic parameters obtained for guinea pigs in this study were compared to those from other species (Table V). The pharmacokinetic parameters were calculated from the data in the literature (22,23) according to the two-compartment open model. In the case of ouabain, the dog is not an appropriate animal model for predicting tissue distribution of ouabain in humans.

As shown in Fig. 2, the time of peak $K_{p,vivo}$ appeared later than 65 min except in brain. Since this later peak of $K_{p,vivo}$ could not be explained by a model assuming rapid equilibrium of tissue distribution, incorporation of a slow binding process may be required to account for the time course of tissue concentration of ouabain. The $K_{p,vivo}$ value was calculated by averaging $K_{p,vivo}$ among 65–725 min. Then the volume of distribution was estimated according to the following equation:

$$V_{d,app} = \sum_{i}^{n} V_{t,i} \cdot K_{p,vivo,i} \qquad (11)$$

where $V_{d,app}$ and $V_{t,i}$ represent the apparent volume of distribution and the tissue volume in each tissue (i), and the values were taken from the literature (24,25). The calculated value of $V_{d,app}$ was 2.38 L/kg, which agreed well with the volume of distribution at steady state ($V_{d\ ss}$; 2.78 L/kg) calculated from the plasma concentration–time curve. The following tissues were the major tissues in ouabain distribution: muscle (84%), GI (6.8%), kidney (4%), and liver (4%).

There is a stoichiometric relationship between ouabain binding capacity and hydrolytic activity of Na,K-ATPase (26,27); therefore, it was possible to quantify the total amount of Na,K pumps in intact cells such as skeletal muscle and fat cells (28) by measuring ^{3}H-ouabain binding *in*

Table II. Binding Parameters of Ouabain for Na,K-ATP in Each Tissue

Tissue	Dissociation constant (nM; Mean ± SE)[a]	Binding capacity (nmol/L of 0.5% homogenate; mean ± SE)[a]
Heart	370 ± 82	3.39 ± 0.47
Muscle	131 ± 35	1.28 ± 0.44
Kidney	260 ± 26	21.5 ± 1.6
Liver	415 ± 150	1.95 ± 0.42
Lung	627 ± 147	1.87 ± 0.69
Brain	188 ± 94	19.2 ± 8.0

[a] Binding experiments were repeated three times for each tissue. Each binding parameter was obtained by the nonlinear least-squares method (18) assuming a single binding site (Eq. 7) as described under Methods.

Table III. Summary of Regression Analysis on $K_{p,vivo}$

Parameter	R^{2a}	a^b	b^c	Significance of regression[d]
V_e/V_t	29.0	5.98	21.8	$P > 0.25$
K_d	29.4	9.23	−0.0126	$P > 0.25$
B_{max}	90.9	1.81	0.475	$P < 0.025$
$K_{p,vitro}$	93.8	1.79	0.618	$P < 0.01$

[a] Coefficient of determination.
[b] Intercept coefficient.
[c] Slope coefficient.
[d] Tested by the analysis of variance test.

Table IV. Comparison of K_p Values *in Vivo* and *in Vitro*

Tissue	V_e/V_t[a]	K_d[b]	B_{max}[b]	$K_{p,vitro}$[c]	$K_{p,vivo}$
Heart	0.30	370	3.39	2.13	4.24
Kidney	0.20	260	21.5	16.7	12.0
Muscle	0.13	131	1.28	2.08	4.01
Liver	0.29	415	1.95	1.23	2.14
Lung	0.38	627	1.87	0.97	0.88
Brain	0.002	188	19.2	20.4	0.18

[a] The ratio of extracellular space to the whole tissue space obtained from the literature (20).
[b] K_d and B_{max} were obtained from an *in vitro* binding study and are summarized in Table III.
[c] Calculated considering the dilution factor, d, according to Eq. (9) as described under Methods.

vitro. In skeletal muscle, the Na,K pump is located in the sarcolemma (29) as well as in the transverse tubuli (30), while the sarcoplasmic reticulum contains no Na,K pumps (31).

In this study, the specific binding of ouabain to Na,K-ATPase was measured using 0.5% tissue homogenate so that the loss of Na,K-ATPase during the preparation of the tissue sample can be minimized. The dissociation constants were of the order of hundreds of nanomolars; on the other hand, the maximum binding capacity varied from 1.28 in muscle to 21.5 in kidney. This 17-fold difference in B_{max} corresponds well with that of $K_{p,vivo}$ (14-fold difference except in brain). Regression analysis indicates (Table III) that the binding capacity was the principal factor of the intertissue variation of $K_{p,vivo}$. In addition, the calculated $K_{p,vitro}$ values, based on the *in vitro* binding parameters, were comparable with $K_{p,vivo}$ (Table IV), which suggests again that ouabain binding to Na,K-ATPase is the major factor in the tissue distribution of ouabain. In brain, $K_{p,vitro}$ is the largest in measured $K_{p,vitro}$, while $K_{p,vivo}$ is the smallest. These differences may be explained as follows: ouabain cannot penetrate the blood–brain barrier but can bind to Na,K-ATPase on the brain parenchymal cell membrane, which can be measured in the *in vitro* binding study using brain homogenate.

Recently, determinant factors in the tissue distribution of several drugs were identified, such as vincristine (32), vinblastine (33), quinidine, propranolol, and imipramine (34). The K_p values of vincristine and vinblastine correlated well with the tissue concentration of tubulin, and the K_p values of weakly basic drugs correlated well with the tissue concentration of phosphatidylserine. However, the constructed $K_{p,vitro}$, based on the *in vitro* experiments, fail to match $K_{p,vivo}$. As far as we know, examples of successful estimation of $K_{p,vitro}$ are those for ethoxybenzamide (35), doxorubicin (7), weakly acidic and basic drugs (36), and ouabain in this study.

The experimental approach presented here provides insights into the mechanism of drug tissue distribution as a basis for predicting drug tissue concentration in humans.

Table V. Summary of Pharmacokinetic Parameters of Ouabain in Mammals

Species	$V_{d\ ss}$ (L/kg)[a]	CL_{tot} (ml/min/kg)[b]	Sampling time (hr)[c]	Ref.
Rabbit	1.38	3.35	12	22
Dog	2.07	2.75	12	22
Guinea pig	2.22	7.06	12	this study
Rat	4.35	7.84	12	22
Human	11.5	9.14	48	23

[a] The plasma disappearance curve was fitted to a two-compartment open model in each case, except for guinea pigs. $V_{d\ ss}$ was calculated as dose $\Sigma_i^3 A_i/a_i^2/AUC^2$ (19).
[b] Calculated as dose/AUC.
[c] The duration of the study.

REFERENCES

1. R. L. Dedrick and K. B. Bishoff. Pharmacokinetics in applications of the artificial kidney. *Chem. Eng. Progr. Symp. Ser.* 64:32–44 (1968).
2. K. B. Bishoff and R. L. Dedrick. Thiopental pharmacokinetics. *J. Pharm. Sci.* 57:1346–1351 (1968).
3. K. J. Himmelstein and R. J. Lutz. A review of the applications of physiologically based pharmacokinetic modeling. *J. Pharmacokin. Biopharm.* 7:127–145 (1979).
4. L. E. Gerlowski and R. K. Jain. Physiologically based pharmacokinetic modeling: Principles and applications. *J. Pharm. Sci.* 72:1103–1127 (1983).
5. R. L. Dedrick. Animal scale up. *J. Pharmacokin. Biopharm.* 1:435–461 (1973).
6. Y. Sawada, M. Hanano, Y. Sugiyama, H. Harashima, and T. Iga. Prediction of the volume of distribution of basic drugs in humans based on data from animals. *J. Pharmacokin. Biopharm.* 12:587–594 (1984).
7. T. Terasaki, T. Iga, Y. Sugiyama, and M. Hanano. Pharmacokinetic study on the mechanism of tissue distribution of doxorubicin: Interorgan and interspecies variation of tissue-to plasma partition coefficients in rats, rabbits and guinea pigs. *J. Pharm. Sci.* 73:1359–1363 (1984).
8. L. I. Harrison and M. Gibaldi. Pharmacokinetics of digoxin in the rat. *Drug Metab. Disp.* 4:88–93 (1976).
9. J. Sato, Y. Sawada, T. Iga, and M. Hanano. Effect of quinidine on digoxin distribution and elimination in guinea pigs. *J. Pharm. Sci.* 72:1137–1141 (1983).
10. D. J. Weidler, N. S. Jallad, H. S. Movahhed, E. Sakmar, and J. G. Wagner. Pharmacokinetics of digoxin in the cat and comparisons with man and the dog. *Res. Comm. Chem. Pathol. Pharmacol.* 19:57–66 (1978).
11. L. I. Harrison and M. Giboldi. Physiologically based pharmacokinetic model for digoxin distribution and elimination in the rat. *J. Pharm. Sci.* 66:1138–1142 (1977).
12. L. I. Harrison and M. Giboldi. Physiologically based pharmacokinetic model for digoxin disposition in dogs and its preliminary application to humans. *J. Pharm. Sci.* 66:1679–1683 (1977).
13. O. Hansen. Interaction of cardiac glycosides with ($Na^+ + K^+$)-activated ATPase. A biochemical link to digitalis-induced inotropy. *Pharmacol. Rev.* 36:143–163 (1984).
14. K. Repke, M. Est, and H. J. Portius. Uber die ursache der speciesunterschied in der digitalisempfindlichkeit. *Biochem. Pharmacol.* 14:1785–1802 (1965).
15. T. Akera, S. I. Baskin, T. Tobin, and T. M. Brody. Ouabain: Temporal relationship between the inotropic effect and the in vitro binding to and dissociation from ($Na^+ + K^+$)-activated ATPase. *Naunyn-Schmiedelberg Arch. Pharmacol.* 277:151–162 (1973).
16. M. Y. Abeywardena, E. J. Mcmurchie, R. Gordon, and J. S. Charnock. Species variation in the ouabain sensitivity of cardiac Na^+, K^+-ATPase. *Biochem. Pharmacol.* 33:3649–3654 (1984).
17. H. Harashima, Y. Sugiyama, T. Iga, and M. Hanano. Nonlinear tissue distribution of ouabain in rabbits. *Drug Metab. Disp.* 16:645–649 (1988).

18. K. Yamaoka, Y. Tanigawara, T. Nakagawa, and T. Uno. A pharmacokinetic analysis program (MULTI) for microcomputer. *J. Pharmacobio-Dyn.* **4**:879–890 (1981).
19. M. Gibaldi and D. Perrier. *Pharmacokinetics,* 2nd ed., Marcel Dekker, New York, 1982.
20. A. Tsuji, T. Yoshikawa, K. Nishide, H. Minami, M. Kumura, E. Nakashima, T. Terasaki, E. Miyamoto, C. H. Nightingale, and T. Yamanaka. Physiologically based pharmacokinetic model for beta-lactam antibiotics I: Tissue distribution and elimination in rats. *J. Pharm. Sci.* **72**:1239–1251 (1983).
21. E. F. Adolph. Quantitative relations in the physiological constitutions of mammals. *Science* **109**:579–585 (1949).
22. J. Q. Russell and C. D. Klassen. Species variation in the billiary excretion of ouabain. *J. Pharmacol. Exp. Ther.* **183**:513–519 (1972).
23. R. Selden and T. W. Smith. Ouabain pharmacokinetics in dog and man. *Circulation* **45**:1176–1182 (1972).
24. P. O. Sjoquist, L. Bjellin, and A. M. Carter. Effect of a vasopressin analogue (N4-glycyl-glycyl-glycyl-(8-lysine)-vasopressin) on organ blood flow in the pregnant guinea pig. *Acta Pharmacol. Toxicol.* **40**:369–377 (1977).
25. L. L. Peters, G. Grutters, and C. B. Martin, Jr. Distribution of cardiac output in the unstressed pregnant guinea pig. *Am. J. Obstet. Gynecol.* **138**:1177–1184 (1980).
26. O. Hansen. The relationship between g-strophanthin-binding capacity and ATPase activity in plasma membrane fragment from ox brain. *Biochim. Biophys. Acta* **233**:122–132 (1971).
27. P. L. Jorgensen and J. C. Skou. Purification and characterization of $(Na^+ + K^+)$-ATPase in preparations from the outer medulla of rabbit kidney. *Biochim. Biophys. Acta* **233**:366–380 (1971).
28. T. Clausen and O. Hansen. Ouabain binding and Na^+-K^+ transport in rat muscle cells and adipocytes. *Biochim. Biophys. Acta* **345**:387–404 (1974).
29. P. V. Sulakhe, M. Fedelesova, D. B. McNamara, and N. S. Dhalla. Isolation of skeletal muscle membrane fragments containing active Na^+-K^+ stimulated ATPase: Comparison of normal and dystrophic muscle sarcolemma. *Biochem. Biophys. Res. Commun.* **42**:793–800 (1971).
30. Y. H. Lau, A. H. Brunschwig, and J. P. Brunschwig. Isolation of transverse tuble by fractionation of triad junctions of skeletal muscle. *J. Biol. Chem.* **252**:5565–5574 (1977).
31. R. A. Sabbadini and V. R. Okamoto. The distribution of ATPase activities in purified transverse tubular membrane. *Arch. Biochem. Biophys.* **223**:107–119 (1983).
32. K. Wierzba, Y. Sugiyama, K. Okudaira, T. Iga, and M. Hanano. Tubulin as a major determinant of tissue distribution of vincristine. *J. Pharm. Sci.* **76**:872–875 (1987).
33. K. Wierzba, Y. Sugiyama, T. Iga, and M. Hanano. Kinetic study on the mechanism of tissue distribution of vinblastine. *J. Pharmacobio-Dyn.* **11**:651–661 (1988).
34. N. Yata, T. Toyoda, T. Murakami, A. Nishiura, and Y. Higashi. Phosphatidylserine as a determinant for the tissue distribution of weakly basic drugs in rats. *Pharm. Res.* **7**:1019–1025 (1990).
35. J. H. Lin, Y. Sugiyama, S. Awazu, and M. Hanano. In vitro and in vivo evaluation of the tissue to plasma partition coefficient for physiological pharmacokinetic models. *J. Pharmacokin. Biopharm.* **10**:637–647 (1982).
36. G. Schuhumann, B. Fichtl, and H. Kurz. Prediction of drug distribution in vivo on the basis of in vitro binding data. *Biopharm. Drug Dispos.* **8**:73–76 (1987).